Structure of a fluid dioleoylphosphatidylcholine bilayer determined by joint refinement of x-ray and neutron diffraction data

III. Complete structure

Michael C. Wiener and Stephen H. White

Department of Physiology and Biophysics, University of California, Irvine, California 92717 USA

ABSTRACT We present in this paper the complete structure of 1,2-dioleoyl-sn-glycero-3-phosphocholine (DOPC) in the L_α phase (66% RH, 23°C) obtained by the joint refinement of neutron and x-ray lamellar diffraction data. The structural details obtained have previously required a large number of neutron diffraction experiments using numerous specifically-deuterated phospholipid isomorphs (Büldt et al., 1978. Nature (Lond.). 271:182–184). The joint-refinement approach minimizes specific deuteration by utilizing independent neutron and x-ray data sets. The method yields a quasimolecular structure consisting of a series of multiatomic fragments that are each represented by one or several Gaussian distributions whose positions and widths can be determined to within 0.06 to 0.52 Å exclusive of the methylene region. The image of DOPC at 66% RH (5.36 ± 0.08 waters per lipid) is consistent with many aspects of bilayer structure previously determined by structural and spectroscopic studies. The most striking feature of the structure is the large amount of transbilayer thermal motion suggested by the widths and overlaps of the Gaussian envelopes of the quasimolecular fragments. We discuss the "dynamic bilayer thickness" which describes the minimum effective thickness of the hydrocarbon permeability barrier in terms of the thermal motion of the water. A gradient of thermal motion exists that increases in either direction away from the glycerol backbone which is the most constrained portion of the bilayer. The steric interactions between headgroups of apposed bilayers, expected at the hydration level of our experiments, are clearly revealed. A useful consequence of the quasimolecular structure is that average boundaries within bilayers calculated using composition and volumetric data and ad hoc assumptions can be related to the positions of the principal structural groups. Several measures of "bilayer thickness" in common use can be identified as the positions of the cholines for Luzzati's d_l (Luzzati and Husson. 1962. J. Cell Biol. 12:207–219) and the glycerols for Small's d_L (Small. 1967. J. Lipid Res. 8:551–556). We do not know if these relations will be true at other hydrations or for other lipids. Of particular interest is the fact that the position of the carbonyl groups marks the average hydrocarbon/headgroup boundary. It must be emphasized, however, that this region of the bilayer must be generally characterized as one of tumultuous chemical heterogeneity because of the thermal motion of the bilayer.

INTRODUCTION

We present in this paper the complete structure of a liquid-crystalline (L_α phase) bilayer formed from 1,2-dioleoyl-sn-glycero-3-phosphocholine (DOPC) as the culmination of our recent investigations of methods for maximizing the information obtainable from lamellar diffraction data from thermally disordered bilayers. Two earlier papers established the theoretical foundations of what we refer to as "liquid-crystallography". The first (Wiener and White, 1991a) examined critically the issue of resolution in membrane diffraction and the role of appropriate models in structural refinement. Quasimolecular models (King and White, 1986) that represent the liquid-crystalline bilayer in terms of a series of multiatomic Gaussian distributions were shown to provide a physically meaningful real-space representation of the distribution of matter in the bilayer. The positions

of each Gaussian describe the most probable location of the center-of-scattering of each quasimolecular fragment while the widths of the Gaussians provide estimates of the range of the thermal motion of each fragment projected onto the bilayer normal. The second paper (Wiener and White, 1991b) described the composition-space refinement method which enables the simultaneous consideration of neutron and x-ray diffraction data in bilayer structure determination. A requirement of the joint-refinement procedure is that the neutron and x-ray structure factors be placed on the appropriate absolute scales (King et al., 1985; Jacobs and White, 1989; Wiener and White, 1991b). This can be done by analysis of diffraction data from structural isomorphs to determine the required instrumental calibration factors (Wiener and White, 1991c; Wiener et al., 1991).

The quasimolecular Gaussian distributions that comprise the structure of DOPC described in this paper were determined by fitting simultaneously structure factors obtained from composition-space structural models to x-ray and neutron structure factors. However, the

---

Address correspondence to Dr. White.

Dr. Wiener's present address is Department of Biochemistry and Biophysics, University of California, San Francisco, California 94143-0448.

transbilayer distributions of the water, double-bonds, and terminal methyl groups used in the models were determined independently in earlier experiments. Neutron diffraction experiments using specific deuteration yielded the water and double-bond distributions and the neutron instrumental scale factors (Wiener et al., 1991). The x-ray instrumental factor was obtained from experiments using specifically brominated DOPC (Wiener and White, 1991c). Once the x-ray and neutron structure factors had been properly scaled, the distribution of the terminal methyl groups could be determined by a direct real-space combination of neutron and x-ray data (Wiener and White, 1992). The specific procedures used to refine the quasimolecular model are described in detail in the present paper. The resultant structure is a fully-resolved image of a liquid-crystalline bilayer observed over the long time-scale of diffraction experiments.

METHODS

Joint refinement method

We have detailed the theoretical (Wiener and White, 1991a, b) and experimental (Wiener and White, 1991c; Wiener et al., 1991) methods that are involved in the joint refinement of liquid-crystalline bilayer structures. The input data for the structure determination are the absolute x-ray and neutron structure factors (Wiener and White, 1991c; Wiener et al., 1991). Thermally-disordered bilayers are adequately described by a series of multiatomic quasimolecular fragments that are each represented in composition-space (Wiener and White, 1991b) by one or several Gaussian distributions

$$n_i(z) = (N_i/A_i\sqrt{\pi}) \exp\left[-(z - Z_i/A_i)^2\right]. \quad (1)$$

The composition-space distribution $n_i(z)$ is the number per unit length or the probability of locating the center-of-scattering of quasimolecular piece i within the bilayer (Wiener and White, 1991b). The center of the distribution is at Z_i and has a $1/e$-halfwidth A_i. The distribution can be viewed as the convolution of the hard-sphere or steric distribution of the quasimolecular fragment with an envelope of thermal motion (Wiener and White, 1991c; Wiener et al., 1991). The average distribution of matter within the bilayer is accurately represented on the diffraction time-scale by a composition-space structure which is mapped to neutron or x-ray scattering space by multiplication of each quasimolecular fragment by the appropriate scattering-length b_{ji}, where j denotes neutron or x-ray scattering length,

$$\rho_{ji}^*(z) = b_{ji} n_i(z). \quad (2)$$

Values of neutron scattering lengths are tabulated by Sears (1986); x-ray scattering lengths for low-angle lamellar diffraction are given by the atomic number multiplied by e^2/mc^2, where m is the electron mass (Warren, 1969). The neutron and x-ray structure factors $F_j(h)$ of the model consisting of the set of p quasimolecular pieces are then given analytically by the Fourier transform of Eq. 2 summed over all of the pieces,

$$F_j(h) = 2 \sum_{i=1}^{p} b_{ji} N_i \exp\left(-(\pi A_i h/d)^2\right) \cdot \cos\left(2\pi Z_i h/d\right). \quad (3)$$

Quasimolecular model (parsing)

Fig. 1 depicts the quasimolecular model of DOPC and its associated water molecules that was used in the structural determination. This one was chosen initially because it logically identified the obvious molecular fragments. We subsequently examined more than 30 other parsing schemes but none of them led to successful refinements. The general principles of parsing the unit cell into quasimolecular fragments has been described elsewhere (Wiener and White, 1991b).

The methylene region (part number 2) in Fig. 1 is represented by three Gaussians so that ten quasimolecular fragments were required to obtain the complete structure of DOPC. Each piece requires three parameters: position Z_i, $1/e$-halfwidth A_i, and area N_i. The water and double-bond distributions were determined independently from neutron diffraction experiments (Wiener et al., 1991) which reduced the number of parameters from 30 to 24. The terminal methyl distribution was determined from a direct combination of neutron and x-ray data before the full joint-refinement (Wiener and White, 1991d) so the parameter set was further reduced to 21. The contents of each of the remaining pieces of the model, except for the methylene envelope, were fixed by the parsing so that only the positions and $1/e$-halfwidths were determined during the nonlinear minimization. Specifically, the contents of the carbonyl, glycerol, phosphate, and choline fragments were fixed so that the number of parameters was reduced to seventeen. The two carbonyl groups were considered as a single fragment despite the fact that they are positionally inequivalent in crystalline and gel phases (see e.g., Hitchcock et al., 1974; Elder et al., 1977; Büldt et al., 1978; Hauser et al., 1981). We have considered this issue elsewhere in the context of the double-bonds (Wiener et al., 1991) and believe that similar arguments hold for the carbonyls; namely, the time-averaged thermal motions associated with the L_α phase obscure any instantaneous positional differences due to motional inequivalence.

Three Gaussian distributions were required to model adequately the methylene region. Because the total scattering length of the three Gaussians is known, the number of free parameters is reduced to sixteen. Eight structure factors each were obtained from neutron and x-ray diffraction experiments so the structure could be determined
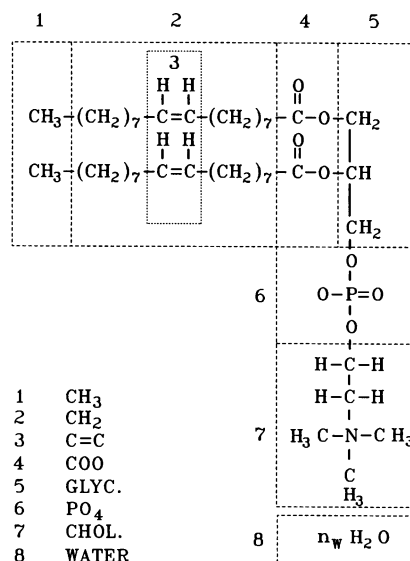

FIGURE 1 The parsing of DOPC into the quasimolecular parts used in the structure determination by the joint refinement of x-ray and neutron data.

solely from the structure factors and the previously determined water, double-bond, and methyl distributions. We estimated previously that a fluid bilayer yielding h_{max} diffraction orders would require $p \sim h_{max}$ quasimolecular Gaussian distributions to describe it adequately (Wiener and White, 1991b). Here we have $h_{max} = 8$ orders for both x-rays and neutrons and $p = 10$ Gaussian fragments consistent with the approximation.

Structure calculation

The structure was determined by finding the set of composition-space models that yielded the best agreement to both the neutron and x-ray data. Nonlinear minimization with the standard Levenberg-Marquardt algorithm (Bevington, 1969; Press et al., 1986) was carried out to determine the parameters Z_i and A_i of Eq. 3 which minimized the joint crystallographic R-factor defined here as

$$R = \sum_{j=n,x} R_j, \tag{4}$$

where

$$R_j = \sum_h \||F_j(h)| - |F_j^*(h)|\| / \sum_h |F_j^*(h)|. \tag{5}$$

$F_j^*(h)$ are the experimental structure factors scaled to the appropriate relative absolute scale (King et al., 1985; Jacobs and White, 1989; Wiener and White, 1991b; Wiener et al., 1991). All calculations were performed on a Sun 4/110 workstation (Sun Microsystems, San Jose, CA). A composition-space structure was judged to be satisfactory if it provided fits to both the neutron and x-ray data sets that were below the experimental noise or "self-R" (Wiener and White, 1991a) values of each set. The final relative absolute self-R factors of the neutron and x-ray data sets are 0.065 and 0.084, respectively (Wiener et al., 1991). The robustness of the structure determination and the uncertainties in the parameters were examined by introducing Gaussian-distributed noise into the data sets. Each of the absolute neutron and x-ray structure factors has an associated uncertainty which was used to define the width of a normal distribution centered at the best value of the structure factor. Monte Carlo methods (Press et al., 1986; Wiener and White, 1991c; Wiener et al., 1991) were used to select mock data from these distributions which were used as the input for the structural calculations.

During our first modeling attempts, only the eight neutron and eight x-ray structure factors were utilized. Structures were obtained that adequately fit both of these data sets; however, the resultant structures produced large higher order ($h > 8$) x-ray structure factors. Scaling the composition-space fragments to x-ray scattering space and summing them to obtain an absolute x-ray density profile yielded profiles that showed substantial high-frequency ringing. This nonphysical behavior was due entirely to the particular form of the three-Gaussian methylene envelope obtained by considering only the eight observed x-ray structure factors and the eight observed neutron structure factors in the analysis. In retrospect, the result that the particular three-Gaussian envelopes obtained originally yielded large amplitude structure factors for $h > 8$ is not surprising because (a) the x-ray scattering length of the methylenes is a significant fraction of the total scattering of the bilayer so the methylene distribution can make non-negligible contributions to the calculated structure factors and (b) no bounds were introduced to constrain higher orders.

However, there is an experimental fact that can be used as a bound on the higher orders: the failure to observe x-ray diffraction orders $h > 8$. The smallest observed x-ray diffraction intensity was used to estimate the threshold values of possible higher-order structure factors that were not observed. Specifically, the eighth order structure factor,

$F(8)$, was observed in x-ray diffraction experiments with exposure times of 24 and 120 h. The observed eighth order intensity for an oriented sample is proportional to $|F(8)|^2/8$, and because this order was observed over a five-fold range of exposures, we estimated the detectable intensity threshold of our experiments to be $\sim |F(8)|^2/40$. Therefore, the threshold value of an x-ray structure factor $F(h), h > 8$, is given by $\sqrt{[h \cdot |F(8)|^2/40]}$. Because we could only estimate the thresholds of the possible intensities, the unambiguous selection of phases or the use of a normal distribution with these pseudo higher order data is not justified. Each possible $h > 8$ x-ray structure factor can have any magnitude between zero and its threshold value and can be of either phase. Therefore, we included five higher order ($h = 9–13$) x-ray structure factors by multiplying each of the threshold values by a random number from a uniform distribution between zero and one and phased them by selecting a random bit. The threshold values of the higher orders provide a bound that constrains the behavior of the methylene envelope. This reinforces the point that there is information in the structure factors that are observed and also in the higher orders that are not observed. We stress that our treatment of the higher order x-ray data as a bound is not a truncation that forces all of the unobserved orders to zero; setting all higher orders to zero is not justifiable based upon the experimental data.

Two sets of structure calculations were performed. In the first [CALC(1)], the eight orders of neutron and x-ray data were fixed at their best values and only the five higher order ($h = 9–13$) x-ray structure factors were varied randomly as just described. The results of 50 successful fits were averaged to yield the parameters characterizing the structure; the standard deviation of each set of 50 parameter values was used as an estimate of the parameter uncertainty. In the second [CALC(2)], the calculation was repeated except that Gaussian noise was introduced into observed x-ray and neutron structure factors ($h = 1–8$) to obtain another fifty successful structures from which standard deviations could be obtained for parameter uncertainties. For the characterization of the methylene envelope that consisted of three Gaussian distributions, real-space averaging was only used to estimate the errors of the parameters but not the parameters themselves. Instead, a set of $h = 1–13$ structure factors were calculated for each of the fifty successful methylene profiles and the fifty values of the structure factor at each order were averaged. The resultant set of averaged structure factors were then fit to a three-Gaussian envelope in reciprocal space to determine the best set of methylene parameter values.

As is typical for virtually all nonlinear minimization problems, the choice of starting parameters (the initial guess) can influence the likelihood of convergence or the particular minima sampled. Exploration of starting parameter values revealed that the minimization was quite robust. Completely arbitrary selection of starting parameters prevented the minimization from converging; conversely, minor variation of starting values had a negligible effect on the final parameter values. Typically, all of the quasimolecular pieces were started with the same 1/e-halfwidth (4 Å). The carbonyl and glycerol were placed at the same position (16 Å) and the phosphate and choline were placed at the same position (20 Å). The methylenes were started at positions $Z = 4$, 8 and 12 Å and each piece started the minimization with 28/3 methylenes. Approximately 10% of the minimizations were successful; the remainder either converged but yielded structure factors that were not within the self-R of one or both of the data sets, or did not converge. The calculated neutron structure factors were frequently not within the self-R of the neutron data which we ascribe to the possibility of inaccuracy in the measurement of the higher order neutron structure factors. However, the total model self-R was always smaller than the observed self-R.

TABLE 1 Neutron and x-ray scattering lengths of the quasimolecular fragments of DOPC (Fig. 1) that were used in the joint refinement structure determination

Piece	N	$b_N^{\parallel}$	$b_X^{\ddagger}$
CH3	2	−0.457	2.540
CH2	28	−0.083	2.257
C=C	2	0.581	3.951
COO	2	1.825	6.208
GLY	1	0.124	6.490
PO4	1	2.834	13.263
CHOL	1	−0.602	14.109
Water	5.36[§]	−0.168	2.822

As in Eq. 1, N is the number of each component in the half-bilayer unit cell. The neutron (b_N) and x-ray (b_X) scattering lengths are in units of 10^{-12} cm. [$\parallel$]Atomic neutron scattering lengths in units of 10^{-12} cm are as follows (Sears, 1986): $H = -0.37390$; $D = 0.6671$; $C = 0.66460$; $N = 0.936$; $O = 0.5803$; $P = 0.513$. [$\ddagger$]Atomic x-ray scattering lengths in units of 10^{-12} cm at low angle are given by the electron number multiplied by mc^2/e^2 (Warren, 1969). [§]White et al. (1987)

RESULTS

Structural parameters

Fig. 1 depicts the parsing used for the quasimolecular model of the DOPC bilayer. As we discussed in an earlier paper (Wiener and White, 1991b) the requirement that a successful quasimolecular model fit two independent sets of data strongly constrains the ways in which the molecule can be divided. While we make no claim that the representation of DOPC in Fig. 1 is unique, it is encouraging that this obvious parsing is the only one out of more than thirty attempted that ade-

quately fit both data sets. The neutron and x-ray scattering lengths of the quasimolecular fragments are listed in Table 1 and the calculated and observed neutron and x-ray structure factors are compared in Table 2. The calculated absolute Fourier density profiles are compared with the experimental results in Fig. 2. While both data sets are adequately fit within their self-R values, the largest deviation is between the calculated and measured first-order neutron structure factor. The calculated structure factor is smaller than the measured value, and this difference is reflected graphically in Fig. 2A by the smaller overall density fluctuation in the calculated profile. We ascribe this disagreement as most probably arising from inaccuracy in the determination of the higher order neutron structure factors which in turn affected the absolute scaling of the neutron data set. Because the higher orders are weak, it is difficult to measure the complete orders over the entire mosaic spread of the oriented multilayer. The method used to extrapolate from the portion of the reflection observed to the entire intensity may have resulted in an overestimate of the higher order values. The 28 month shutdown of the High Flux Beam Reactor at Brookhaven National Laboratory (Upton, New York) precluded the possibility of improving the accuracy of the higher orders through additional experiments. However, there are two points to stress in the comparison of the calculated and observed neutron structure factors. First, the overall agreement between model and experiment is satisfactory in the appropriate context of the experimental neutron self-R of 6.5%. Second, fitting a single structural model to two independent absolute data sets is a very

TABLE 2 A comparison between the experimental and calculated relative absolute neutron and x-ray structure factors $F^*(h)$ for the observed orders of diffraction determined for oriented multilayers of DOPC bilayers at 66% RH

h	OBS[‡]	CALC(1)	CALC(2)	OBS[‡]	CALC(1)	CALC(2)
		Neutron diffraction			X-ray diffraction	
1	−8.00 ± 0.44	−7.16	−7.16	−43.95 ± 0.88	−44.04	−43.97
2	−4.51 ± 0.24	−4.40	−4.41	−0.52 (+0.52, −0.74)[§]	−0.46	−0.64
3	4.81 ± 0.25	4.59	4.60	5.15 ± 0.80	5.31	5.34
4	−5.18 ± 0.29	−5.31	−5.36	−11.97 ± 1.29	−12.00	−12.15
5	−0.59 ± 0.08	−0.56	−0.49	3.38 ± 0.32	3.56	3.77
6	0.84 ± 0.11	0.84	0.80	−2.47 ± 0.88	−2.59	−2.80
7	0.0 ± 0.08	−0.01	−0.05	2.03 ± 0.65	1.99	2.04
8	−0.94 ± 0.14	−0.98	−0.91	−2.24 ± 0.49	−1.92	−1.94
R	0.065	0.055	0.062	0.084	0.014	0.022

The two columns of calculated structure factors, CALC(1) and CALC(2), are for the two types of structure calculation performed (see text). For CALC(1), the mean values of the experimental structure factors were fixed and only the hypothetical higher order ($9 \le h \le 13$) x-ray structure factors were varied. For CALC(2), all of the structure factors were varied as described in the text. The calculated structure factors are for the average structures determined from fifty successful fits. The d-spacing of DOPC at 66% RH is 49.1 ± 0.3Å (Jacobs and White, 1989). [‡]Wiener et al. (1991); [§]The calculated error for the second order is ±0.74, which implies that $F^*(2)$ could actually be positive (−0.52 + 0.74). Because the independent phasing of the structure factors determined the phase of the second order to be −1 (Wiener and White, 1991c), the quoted error is reduced to indicate the exclusion of positive values of F*(2).
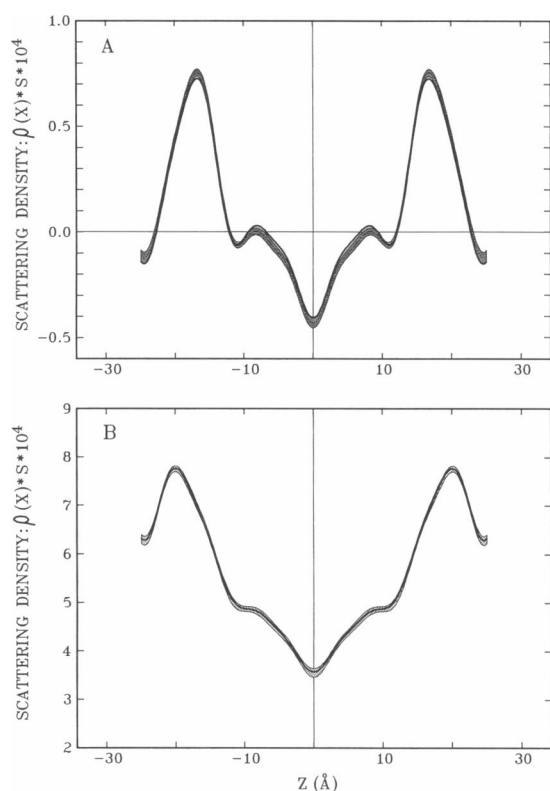
FIGURE 2 Comparison of observed and calculated eight-order absolute scattering length density profiles. The units, scattering length per unit length, are dimensionless and the density scale is multiplied by 10^4. The solid lines are the calculated profiles and the curves with shading show the experimentally determined profiles including experimental error. (A) Neutron density profiles. (B) X-ray density profiles. The ordinate values for x-ray data, without the 10^4 factor, can be converted to electron density (e/$\AA^3$) by dividing by 16.73. This factor includes the 10^4 factor, e^2/mc^2 to convert from scattering length to electrons (Warren, 1969), and the lipid area of 59.3 ± 0.7 $\AA^2$ that was previously determined (Wiener and White, 1992).

FIGURE 3 Composition-space structure of DOPC. (A) The pieces corresponding to the bilayer interior: methyls, methylenes, double-bonds, carbonyls, and glycerol backbone. (B) The headgroup region: phosphate, choline, and water. The methylene region is also indicated.

rigorous test of experimental accuracy. The result that a satisfactory composition-space structural model was obtained that satisfied neutron and x-ray data that were acquired by several people using many different samples over the course of several years is very encouraging to us. Our general experience with the stringency of the refinement shows the importance of accurate structure factor determination.

The complete structure of DOPC at 66% RH is shown in Figs. 3 and 4. Fig. 3 A depicts the structure excluding the headgroup (phosphate and choline) and water distributions. Fig. 3 B shows the headgroup and water distributions and the overlap with the methylene distribution. Fig. 4 shows two bilayer leaflets head-to-head with the water, phosphate, choline, glycerol, and carbonyl fragments indicated. The composition-space pro-
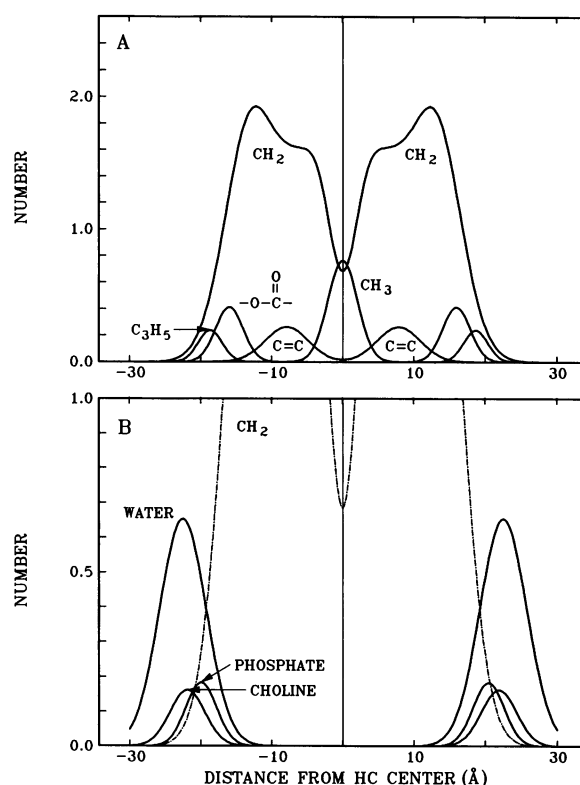
files presented are the average of fifty successful structures obtained by introducing the appropriate noise into all of the data as discussed in the previous section. The parameters of the structure are tabulated in Table 3
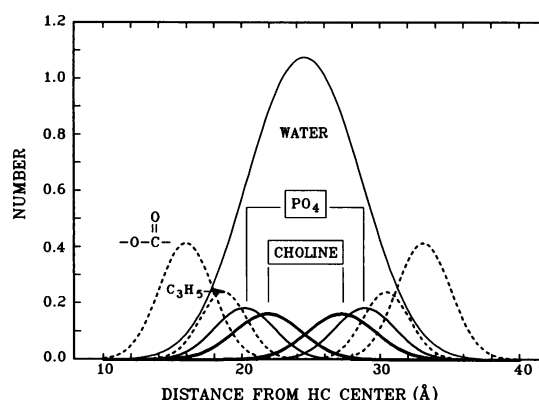

FIGURE 4 Composition space structure of two apposed DOPC leaflets. The overlap of the cholines, and to a lesser extent of the phosphates, is clearly indicated. Water is seen to penetrate the bilayer to the extent of the glycerol backbone fragment.

| Piece | CALC(1) | | CALC(2) | |
	Mean	±SD	Mean	±SD
Z_{CH3}	0.0			
A_{CH3}*	2.95	0.28		
Z_{iCH2}	2.97	0.79	2.95	0.77
A_{iCH2}	2.74	0.80	2.84	0.63
N_{iCH2}	2.74	3.14	3.67	2.64
Z_{mCH2}	5.86	1.63	6.09	1.43
A_{mCH2}	4.21	0.90	3.88	1.04
N_{mCH2}	8.51	2.43	7.18	2.58
Z_{oCH2}	12.85	0.57	12.76	0.59
A_{oCH2}	5.14	0.39	5.19	0.45
N_{oCH2}	16.75	2.32	17.15	2.51
$Z_{C=C}$†	7.88	0.09		
$A_{C=C}$	4.29	0.16		
Z_{COO}	15.97	0.02	15.99	0.06
A_{COO}	2.73	0.05	2.77	0.12
Z_{GLYC}	18.67	0.38	18.67	0.42
A_{GLYC}	2.37	0.31	2.46	0.38
Z_{PO4}	20.19	0.08	20.15	0.13
A_{PO4}	3.08	0.08	3.09	0.16
Z_{CHOL}	21.89	0.13	21.86	0.22
A_{CHOL}	3.48	0.55	3.48	0.52
Z_{WATER}†	22.51	0.77		
A_{WATER}	4.63	0.48		

As in Table 2, the results for the two types of structure calculation described in the text, CALC(1) and CALC(2), are presented. The subscripts identifying the pieces correspond to those in Fig. 1. The symbols i, m, and o used with the methylene (CH2) fragments denote inside, middle, and outer with respect to the bilayer center. *Determined from a direct combination of the neutron and x-ray data prior to the full-joint refinement (Wiener and White, 1992). †Determined from neutron diffraction experiments prior to the full joint refinement (Wiener et al., 1991).

where we include the results of both sets of calculations: CALC(1) for which the neutron and x-ray structure factors were fixed at their mean observed values for $h = 1$–8 while varying the putative $9 < h < 13$ x-ray structure factors using uniform random numbers and CALC(2) for which all structure factors were varied using normally distributed random numbers except for $9 < h < 13$ which were varied as in CALC(1). As expected, the uncertainties are somewhat larger when all of the data have noise introduced. Our subsequent discussion will utilize this latter structure [CALC(2), Table 3]. Based upon model calculations (Wiener and White, 1991a), the quasimolecular fragments that make the largest contributions to the total scattering are most accurately determined in the structure determination. This prediction is verified by the present results. The major contributors to x-ray and neutron scattering, respectively, are the phosphate and carbonyl regions and these are seen in Table 3 to be determined most accurately. The sensitivity limit of the structure determi-

nation is approximately that of the glycerol backbone which makes minor contributions to both the x-ray and neutron scattering.

The methylene distribution presented a slightly different situation in the analysis. A three-Gaussian envelope was required, where only the total number of methylenes (28) was constrained. Because we only constrained the total area of the envelope, the set of three-Gaussian profiles that yield the envelope is degenerate so that the individual constituent Gaussians have no unique physical meaning. The conserved unique sum of the Gaussians representing the long time-averaged shape of the methylene envelope is meaningful, however. Fig. 5 shows the real-space average of the fifty methylene profiles for a single lipid determined during the refinement; the conservation of the shape of the total methylene envelope demonstrates the robustness of the result. Although the methylene region contributes a major fraction of the total x-ray scattering, it is spread out over a wide range so its effective contribution is reduced. While the contribution of a quasimolecular fragment to a structure factor is proportional to its total scattering length, the width of the distribution appears as an exponential factor that dominates the structure factor amplitude (Eq. 3).

We have previously examined the issue of the resolution of quasimolecular models used in liquid-crystalline bilayer structure determination (Wiener and White, 1991a). While carrying out model calculations, we observed that the resolution obtainable from modeling decreases at the edges of the unit cell. Conversely, variation in the position of a quasimolecular fragment near the edge of the unit cell has less of an influence on the structure factor than variation at other positions in
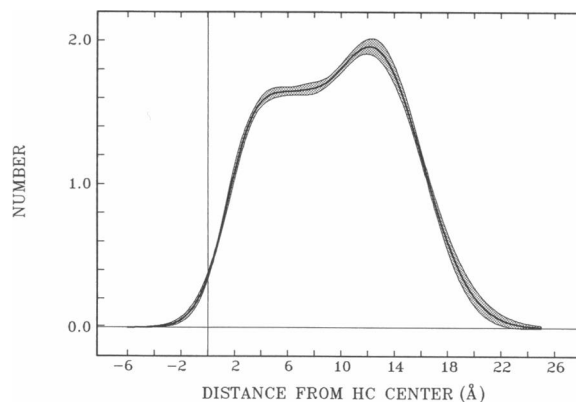

FIGURE 5 Composition-space averaged methylene envelope. Although the three-Gaussian basis set that comprises the methylene distribution is degenerate, the resultant sums of the three Gaussians are conserved.

the unit-cell interior. This effect was observed in the joint refinement of DOPC. Many of the fits that converged but yielded errors above the observed self-R value of the neutron data placed the glycerol and/or choline fragments close to or at $d/2$, where d is the lamellar repeat of 49.1 ± 0.3 Å (Jacobs and White, 1989). Also, there were a small number of structures that fit both sets of data satisfactorily but positioned the glycerol fragment at or near $d/2$. We introduced a single structural constraint to filter out this anomalous result. If a composition space structure provided a successful fit to both neutron and x-ray data, the difference between the positions of the glycerol and carbonyl pieces was calculated. If this difference was greater than or equal to 5 Å, a limit estimated from CPK molecular models, then the structure was not considered successful and was discarded. Only ~ 10% of the structures that fit both sets of data had this feature of a nonphysical carbonyl–glycerol separation; except for this sole distance constraint, the structure determination was a completely free fit.

Bilayer undulations

We have assumed in the quasimolecular modeling that the $1/e$-halfwidths of the Gaussians are due only to thermal fluctuations relative to a bilayer's mean position. This will be true only if there are no whole-body fluctuations of the individual bilayers. This assumption is not valid for liquid crystalline systems with very flexible lamellae as shown elegantly by Smith et al. (1987), Sirota et al. (1988), and Safinya (1989). Depending upon their elastic properties, the lamellae may undergo undulations which result in fluctuations around the mean positions with mean-square amplitude $\langle u^2 \rangle$. Therefore, it is important to consider the possibility of contributions to the Gaussian envelopes from these motions in our system. The mean-square amplitude of the undulatory fluctuations is given by

$$\langle u^2 \rangle = d^2 \eta_1 \ln (L/a)/2\pi^2, \qquad (6)$$

where d is the bilayer repeat, L the characteristic thickness of the sample, and a the in-plane interparticle distance (Sirota et al., 1988). The parameter η_1 describes the stiffness of the membrane and may be determined from the lineshapes of the diffraction peaks. Smith et al. (1987) have examined the line shapes for diffraction peaks from L_α-phase dimyristoylphosphatidyl-choline (DMPC) at 90% RH and determined that $\eta_1 \approx 0$ but could not rule out a value as large as 0.0016 because of experimental uncertainty based upon the $h = 8$ diffraction peak. We can therefore establish an upper limit for $\langle u^2 \rangle$ for our experiment. Using $d = 49.1$ Å, $L = 10$ μm (Wiener and White, 1991c), and $a = 8.7$ Å

(estimated from $\pi(a/2)^2 = S = 59.3$ Å^2 [Wiener and White, 1991d]), Eq. 6 yields $\langle u^2 \rangle = 1.8$ Å^2 or $u_{\text{rms}} = 1.4$ Å. For comparison with our data, we use the undulatory $1/e$-halfwidth $A_U \equiv \sqrt{2} \cdot u_{\text{rms}} = 2.0$ Å. We emphasize that this is an upper limit. Because our measurements were made at a lower relative humidity than those of Smith et al. (1987), we expect η_1 to be smaller than this.

To compare this estimate with our results, consider the halfwidth of the glycerol fragment which has the smallest halfwidth observed ($A_{\text{GLYC}} = 2.46$ Å, Table 3). Using the approximation $A_{\text{GLYC}} \approx \sqrt{(A_H^2 + A_T^2)}$ discussed elsewhere (Wiener and White, 1991c; Wiener et al., 1991), we estimate that the halfwidth of the thermal envelope $A_T \approx 1.5$ Å for an effective hard-sphere radius $A_H \approx 2.0$ Å. A_T thus has a value comparable to the estimated upper limit of A_U. However, it seems very unlikely to us that the motion of the glycerol is due solely to undulatory motion. This would require the glycerol to be at rest relative to the bilayer which is inconsistent with DOPC being in a fluid state. But what portion of A_T might be due to the whole-body undulations? This can be addressed by considering the x-ray crystallographic Debye-Waller factors (U_{iso}) for the crystal structure of dilauroylphosphatidylethanolamine (DLPE) determined by Elder et al. (1977). The values of U_{iso} for the acyl chain carbons yield $1/e$-halfwidth values of $A_T \approx 0.4$ Å for the C(2) carbons and 0.7 Å for the terminal methyls. Neutron diffraction measurements on specifically deuterated dipalmitoylphosphatidylcholine (DPPC) in the $L_{\beta'}$ phase, which should be stiffer than the L_α phase, yield $1/e$-halfwidths of 1.3 ± 0.6 Å for the C(2) carbon on the acyl chain in the 1 position and 3.0 ± 0.6 Å for the CH$_2$ adjacent to the N(CH$_3$)$_3$ group (Büldt et al., 1979). Synchrotron x-ray reflectivity studies of the air/water interface yield surface roughness factors from which A_T for water molecules is calculated to be 4.0 Å (Als-Nielson, 1987). Similar measurements for eicosanoic acid monolayers at the air/water interface (area/lipid = 22.7 Å^2) yield $A_T = 4.1$ Å (Als-Nielson and Kjaer, 1989). Given these values compared to that for the glycerol in fluid DOPC, it seems unlikely that whole-body undulations make a significant contribution to A_T. We therefore suggest that η_1 is likely to be considerably smaller than its estimated upper limit and that the motions we observe are due almost entirely to thermal motions relative to the mean position of the bilayer.

DISCUSSION

General structural features

The structure of liquid-crystalline L_α-phase DOPC at 66% RH (5.4 waters/lipid) shown in Fig. 3, Fig. 4, and

Table 3 is the complete and fully-resolved image of the bilayer as seen over the diffraction time-scale. The combination of the two independent x-ray and neutron data sets precludes the necessity of copious specific deuteration that was previously required for detailed determination of structural features by neutron diffraction (Büldt et al., 1978, 1979; Zaccai et al., 1979). The image of the bilayer obtained is consistent with the wealth of information gathered over the past decades by spectroscopic and structural methods. Importantly, however, the structural image obtained here is based entirely upon the absolute neutron and x-ray structure factors.

Fig. 6 depicts a space-filling representation of a conformation of DOPC produced using molecular graphics software (BIOGRAF by Molecular Simulations, Inc., Sunnyvale, CA) that is consistent with the positions Z_i of the quasimolecular fully-resolved structure. Although the structure determined by the joint refinement is the average over a large number of conformations, we include Fig. 6 to demonstrate that the positions of the composition-space quasimolecular fragments are consistent with a reasonable structural image of a fluid bilayer. What the static picture in Fig. 6 does not convey is the range of motion of each of the quasimolecular groups arising from the high thermal disorder of the L_α phase. The actual ensemble of molecular conformations yields the composition-space envelopes that we obtained.

An approximate average tilt-angle of the phosphocholine dipole with respect to the bilayer surface can be estimated from the distance between the centers of the phosphate and choline pieces along the bilayer normal. Assuming that the phosphorus and nitrogen atoms are the centers-of-scattering of each of these roughly spherical fragments and a phosphate–nitrogen distance of 4.5
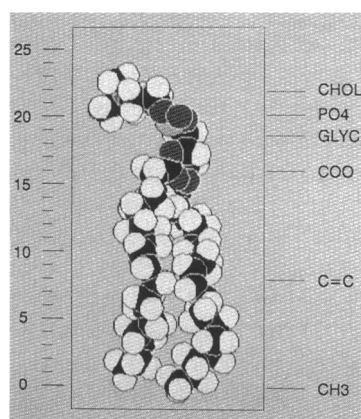

FIGURE 6   A space-filling representation of a DOPC conformer that is consistent with the quasimolecular structure obtained by the joint refinement procedure. The image was made with BIOGRAF (Molecular Simulations, Sunnyvale, CA) on a Sun 4/110 workstation.

Å obtained from the crystal structure of DMPC (Hauser et al., 1981), the dipole is calculated to be canted with an angle of 22 ± 4° with respect to the bilayer surface. This compares favorably with the values obtained from crystal structures (Hauser et al., 1981) and neutron diffraction of oriented multilayers (Büldt et al., 1979) and is in reasonable agreement with the recent value of 18° obtained from ^{2}H-NMR and Raman spectroscopic studies of L_α-phase DPPC (Akutsu and Nagamori, 1991).

In bilayers at reduced hydration, steric factors are believed to play a major role in interbilayer interactions (McIntosh et al., 1987). Fig. 4 shows clear evidence of steric effects between apposed bilayers at the moderate hydration of our experiments. There is significant overlap between the choline distributions and, to a lesser extent, between the phosphate distributions of the two head-to-head bilayer leaflets. In projection, there are regions of space that are accessible to both headgroups, i.e., the position of the headgroup of one bilayer can affect or exclude the other's position. A question of obvious interest is how this steric interaction, clearly seen as an overlap of apposed headgroups in Fig. 4, will change as the hydration level increases. Determining fully-resolved structures over a range of hydration will provide valuable information on this issue and others pertaining to the hydration force (McIntosh and Simon, 1986; Rand and Parsegian, 1989).

Thermal motion

Because the real-space image is physically meaningful, there is useful and interesting information in the widths of the Gaussian distributions that characterize each quasimolecular fragment. The positions of the distributions denote the most likely place to locate the center of scattering of each fragment whereas the widths describe the range of thermal motions projected onto the bilayer normal assuming undulatory motions are insignificant in our system (see Results). The 1/e-halfwidth A_i of a quasimolecular Gaussian fragment can be viewed as the convolution of a hard sphere of van der Waals radius A_H located at Z_i with a Gaussian envelope of thermal motion describing the range over which that piece moves within the bilayer. As discussed earlier in Results, the observed 1/e-halfwidth is given approximately by $(A_H^2 + A_T^2)^{1/2}$ where A_T describes the envelope of thermal motion. Because of the approximate nature of this crude expression and the ambiguity in estimating hard-sphere widths of each of the quasimolecular fragments, we do not explicitly repeat the calculation for all of the fragments.

The narrowest thermal distribution is that of the glycerol region (A_{GLYC} = 2.46 ± 0.38 Å, Table 3). The 1/e-halfwidths of the quasimolecular pieces on either side of the glycerol backbone increase as shown graphi-

cally in Fig. 3 A (see also Fig. 8 A). The general image is a gradient of thermal motion within the interface zone in which the regions bounding the relatively rigid glycerol backbone undergo increasing ranges of motion that are roughly proportional to the distance from the glycerol fulcrum. This is consistent with NMR results (Strenk et al., 1985; Braach-Maksvytis and Cornell, 1988) and crystallographic measurements (Hitchcock et al., 1974; Elder et al., 1977) which indicate that the glycerol backbone is the most rigid portion of glycerophospholipid molecules in liquid-crystalline phospholipid bilayers. It is interesting in this context that the glycerol region is at the extreme boundaries of both the methylene (Fig. 3 A) and water distributions (Fig. 4) and thus marks the water–methylene interface (see also Fig. 9). The net thermal motions within the hydrocarbon region, compared to the interface zone, are qualitatively different in that the 1/e-halfwidth of the terminal methyl groups (2.95 Å) is about the same as the carbonyl (2.77 Å) or phosphate groups (3.09 Å) whereas the width of the double-bond distribution is significantly larger (4.29 Å). This apparent violation of the notion of a gradient of thermal motion may be explained if one treats the flexible acyl chain as being tethered at one end to the interface by the carbonyls and at the other end to the bilayer center by the terminal methyls. Because the half-thickness of the hydrocarbon is considerably shorter than the length of the fully extended chain, the tethering would permit the double-bonds to diffuse over a relatively large volume of space. It would also permit some of the methylenes to venture beyond the C(2) carbons into the interfacial zone (vide infra).

A stringent refinement test

A possible use of the structures determined by the joint refinement is to attempt to determine the precise distribution of physical and chemical properties across the bilayer. Just as the composition-space Gaussians that comprise the structure can be mapped into x-ray or neutron scattering space, they can in principle be mapped into the space of any other intensive thermodynamic quantity (Wiener and White, 1991b). This general idea can also be used to estimate the cross-sectional area $S(z)$ of the lipid at each point z in the bilayer. If the data are perfect, and if the CH_2 volume is independent of position, then this area function must be independent of z (i.e., constant). Scaling the quasimolecular distributions $n_i(z)$ (units of number per unit length) that comprise the composition-space structure by their respective molecular volumes V_i yields the cross-sectional area $S(z)$,

$$\sum_{i=1}^{P} n_i(z)V_i = S(z) \equiv S_0. \tag{7}$$

Because $S(z)$ must be constant across the bilayer, this calculation provides a stringent overall test of the data used in the quasimolecular model.

We calculated $S(z)$ from Eq. 7 using the average composition-space structure [CALC(2)] whose parameters are given in Table 3. The quasimolecular volumes V_i were derived from our analysis and from results in the literature. The volumes of methyls and methylenes are 54 and 27 Å³, respectively (Tardieu et al., 1973; Nagle and Wiener, 1988; Wiener and White, 1992). The volume of each double-bond, which can be obtained by examining alkene volumetric data (Requena and Haydon, 1975), is 43 Å³. Small (1967) estimated that the phosphocholine moiety has a volume of 204 Å³. Because the 1/e-halfwidth of the phosphate is comparable to its van der Waals radius, implying a limited range of thermal motion, we chose to use the volume of lithium phosphate, 70 Å³ (Weast, 1981), as an estimate for the phosphate volume. We note that if phosphoric acid is used as the basis for a volume estimate, then the phosphate volume increases by approximately 20 Å³ but the overall $S(z)$ profile is negligibly affected. The choline volume is then 134 Å³. Nagle and Wiener (1988) estimated the combined volumes of the phosphocholine, carbonyls, and glycerol backbone to be 348 Å³. Combining this volume with Small's result yields a combined volume of the carbonyls and glycerol equal to 144 Å³. Our results on the composition-space glycerol distribution indicate that it is a fairly rigid portion of the lipid molecule so we approximate its volume as the sum of three methylene volumes where the volume of methylenes in the phospholipid subgel phase, 24 Å³ (Nagle and Wiener, 1988), is used. Subtracting the glycerol volume of 72 Å³ leaves a carbonyl volume of 72 Å³ (36 Å³ per carbonyl). Finally, each water molecule has a volume of 30 Å³. The sum of the volumes of the individual pieces, excluding water, is equal to 1,298 Å³. Our measurement of the absolute specific volume of DOPC (Wiener and White, 1992) yields a DOPC volume of 1,295 Å³ which is in good agreement with the derived volume.

We calculated $S(z)$ at 0.5 Å intervals by means of Eq. 7 using the volumes described above and the structural parameters from Table 3 for the CALC(2) calculation. The average value of $S(z)$ is 59.4 Å² which compares favorably with $S_0 = 59.3 \pm 0.7$ Å² determined by Wiener and White (1992) from specific volume measurements. However, as shown in Fig. 7, $S(z)$ is clearly not invariant with respect to z. The standard deviation of $S(z)$ over the bilayer half is ± 4.4 Å² corresponding to apparent variations of $\sim 15\%$ in the cross-sectional area. This variation, seen directly as the peaks and troughs in Fig. 7, is probably due to the uncertainties in the higher order neutron structure factors discussed earlier. Although we cannot absolutely rule out the possibility that the varia-
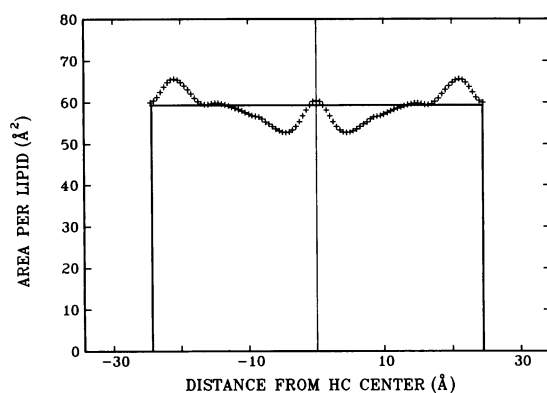
FIGURE 7 Area per lipid [$S(z)$] as a function of position z. Eq. 7 was used with values of the constituent fragment volumes from the literature (see text) to calculate this profile. The horizontal line is the value of S_0 determined from volumetric and hydration measurements (Wiener and White, 1992). As discussed, the positive and negative area fluctuations of $S(z)$ about the experimentally determined value of S_0 correspond to apparent volume fluctuations of $\sim \pm 40$ Å^3, which is a small fraction of the total volume of the unit cell (1,456 Å^3). These apparent fluctuations are indicative of uncertainties in the high-order neutron data and illustrate the stringency of $S(z)$ as a test of the data.

tion in $S(z)$ might be due to a dependence of CH_2 volume on position along the chain (Small, 1986), we think this is unlikely. In any case, this calculation indicates that the physical requirement that $S(z)$ be invariant with respect to z is a very stringent one. The uncertainties implied by these variations should, however, be considered in the proper context. The peaks and troughs in Fig. 7 represent positive and negative variations of the cross-sectional area $S(z)$ from its average value. Integrating each of these regions with respect to the baseline value of the average area (59.4 Å^2, *solid line* in Fig. 7) yields volumes of $\approx +40$ and -40 Å^3, respectively. Forty cubic Å is less than the volume of two methylenes ($V_{CH_2} = 27$ Å^3) and is a small fraction of the total volume (1,456 Å^3) of the half-unit cell. A slightly different set of absolute x-ray and neutron structure factors could yield a slightly different methylene envelope that flattens out this feature in the $S(z)$ profile. Future experiments will eliminate this variation, indicate that the result presented here are at the limits of current experimental accuracy, or possibly reveal variations of CH_2 volume along the acyl chain. This study has repeatedly demonstrated to us that the joint refinement approach relies strongly on the accuracy of experimental data to an extent not previously anticipated nor utilized in most membrane diffraction studies. The obverse of this statement is that the joint refinement yields structural information at a level that has heretofore been quite inaccessible.

Volumetric measures of bilayer thickness

Useful bilayer thickness information has been obtained in the past by using simple equations which use density and volume data to calculate the thickness of a uniform slab of bilayer material. Given S_0 (the area/lipid), the equivalent-slab thickness of a component(s) of the bilayer of molecular volume V is V/S_0. The several methods of this type which are in common use make various assumptions about which parts of the lipid molecule are included in V for the calculation of a bilayer thickness. Small (1967) excluded the phosphocholine group to obtain a lipid thickness d_L of egg lecithin bilayers assumed to be equivalent to a slab of 2 diacylglycerols. Luzzati and his co-workers (Luzzati and Husson, 1962; Luzzati, 1968) included the entire phospholipid molecule to arrive at a bilayer thickness d_ℓ. Nagle and Wiener (1988) extended these slab models to include phospholipid bilayers under a variety of physical conditions to obtain, among other parameters, the idealized hydrocarbon thickness $2D_C$ which is calculated from the volumes of the acyl chains excluding the carbonyl groups. If the average widths of regions of the bilayer obtained from simple volumetric formulae correspond to positions of quasimolecular fragments obtained from joint refinement, then these volumetric methods could be utilized in future studies to constrain further the joint refinement procedure.

To examine this possibility, we calculated the various thicknesses and found that $(d_L/2) = 18.4 \pm 0.2$ Å and $(d_\ell/2) = 21.8 \pm 0.2$ Å which are close to the positions (Table 3) of the glycerol and choline, respectively. Interestingly, the mean of $(d_L/2)$ and $(d_\ell/2)$ is 20.1 Å corresponding closely to the position of the phosphate group. These various correlations are shown graphically in Fig. 8 A. While we do not know if these correlations will be observed at other hydrations or for other lipids, the results are encouraging. Furthermore, they make sense within the context of the assumptions underlying the slab-boundary calculations and thereby give further credence to our determined structure.

Headgroup–hydrocarbon boundary

In the absence of other structural information, the boundary between hydrocarbon and headgroups has generally been taken as the edge of the equivalent slab comprised of the acyl chains beginning with the C(2) carbons (Requena and Haydon, 1975; Lewis and Engelman, 1983; King et al., 1985; White and King, 1985; Scherer, 1989) so that the hydrocarbon thickness ($2D_C$) calculated in the manner of Nagle and Wiener (1988) was assumed to mark the positions of this boundary. The
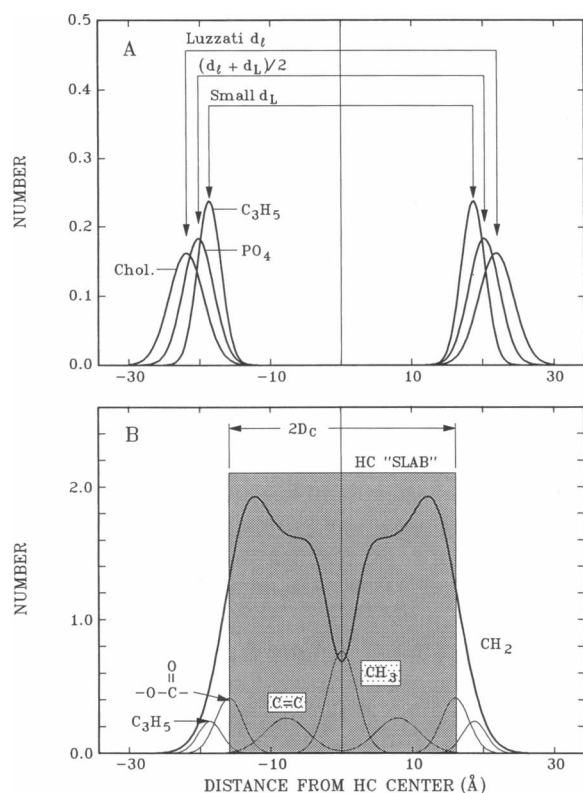
FIGURE 8 Comparisons of volumetric structural features with the refined quasimolecular structure of a DOPC bilayer. (*A*) Comparison of the Luzzati (1968) d_ℓ and Small (1967) d_L values of bilayer thickness. These two thicknesses correspond to the transbilayer separations of the choline and glycerol groups respectively. The mean of d_ℓ and d_L corresponds to the transbilayer separation of the phosphate groups. (*B*) The equivalent hydrocarbon slab (shaded area) of thickness $2D_C$ superimposed on the quasimolecular structure. The edges of the slab correspond to the positions of the carbonyl groups.

equivalent hydrocarbon slab of thickness $2D_C$ has been superimposed on the quasimolecular model in Fig. 8 *B* and it can be seen that the slab edges correspond rather precisely to the positions of the carbonyl groups. Assuming the volumes of the methylenes, double-bonds, and methyls to be 27, 43, and 54 Å^3, respectively, D_C is found to be 16.0 ± 0.2 Å compared to $Z_{COO} = 15.99 \pm 0.06$ Å.

The mean position of the carbonyls is the most accurately determined position of the quasimolecular model because it is the most strongly scattering feature in neutron diffraction experiments. Because the mean position of the C(2) carbons is constrained by the covalent carbonyl–C(2) bond not to exceed 1.54 Å, the measurement of King and White (1986) which places the position of the C(2) carbons at $z = \pm 13.8 \pm 0.25$ Å or 2.2 Å from the carbonyls is probably in error by ~ -0.7 Å. Although the precise separation between the carbonyl and C(2) is thus uncertain, it is reasonable to assume

that the average position of the C(2) is on the hydrocarbon side of the carbonyl rather than the phosphorylcholine side. This suggests that the average direction of the axis through the $-O-CO-CH_2-$ segments will tend to be parallel to the bilayer normal causing the C=O bond to tend to be parallel to the bilayer plane. This general arrangement has been observed in oriented L_α-phase dimyristoyl- and dipalmitoylphosphatidylcholine multilayers by Hübner and Mantsch (1991) by means of FT-IR spectroscopy. Those authors also reported, however, that the orientations of the $-O-CO-CH_2-$ segments at the *sn*-1 and *sn*-2 positions were different but our structure provides no information on this point.

Although the positions of the carbonyls mark the hypothetical hydrocarbon slab boundaries, such boundaries belie the chaotic nature of the interface and, in reality, do not apparently include all of the methylenes. The average number of methylenes extending beyond the slab edges is equal to the area between the methylene envelope and slab boundary in Fig. 8 *B* which is 3.7 or about two methylene groups per hydrocarbon chain. Interestingly, this number is about equal to the average number of methylenes one expects to be exposed to water when the area per lipid increases from 40 Å^2 in the crystalline all-*trans* state to 60 Å^2 in the L_α phase. Aveyard and Haydon (1965) estimated the cross-sectional area of a single methylene group projected onto a plane interface to be 6 Å^2 so that an excess area of 20 Å^2 corresponds to about 3.3 methylenes. Because the average position of the C(2) carbons is displaced from the carbonyl in the direction of the bilayer center (King and White, 1986), these methylenes cannot be attributed entirely to the C(2) carbons and must therefore generally be from more distant carbon positions. This observation would seem to place definite constraints on the allowable chain conformations and is consistent with the idea mentioned earlier that the chains may behave as though they are tethered at each end.

Bilayer thickness dynamics and permeability

We believe that the most important observation of this work is the extent of the transbilayer thermal motion of the quasimolecular fragments which must be taken as a fundamental property of fluid bilayers. There is significant overlap between the distributions that comprise the bilayer so that various regions of the bilayer, such as the headgroup/water interface, consist of a dynamic mixture of components with very different physical and chemical properties (Jacobs and White, 1989). The static image of the bilayer implicit in slab representations can now be replaced with a realistic dynamic image. This image allows one to think more clearly about the problem of

how molecules in the aqueous phase can penetrate the bilayer. Because of the thermal motion, there can be a higher probability of polar molecules such as water penetrating, at least transiently, deeper into the hydrocarbon core than expected on the basis of slab models. This means that the thickness of the bilayer is dynamic with respect to the transbilayer separation of water. This situation is shown in Fig. 9 where we have plotted the distributions of the methylenes, glycerols, double bonds, and water. An important feature of this plot is the small but significant overlap of the water and double-bond distributions indicated by the vertical lines. This overlap suggests to us that there must be transient contacts between the double-bonds and water which may play a role in water permeation of the bilayer. Petersen (1983) has inferred from permeability studies of black lipid films that a single unsaturated bond dramatically increases the solubility of water suggesting an association of water with double bonds. Noting in Fig. 9 that there is a small overlap of the double-bonds at the bilayer center, we can speculate that the double bonds might ferry water across the bilayer.

If one takes the maximum extent of water permeation

into the bilayer as a measure of the minimum transient thickness (which we shall call the dynamic thickness) of the bilayer, the large arrow in Fig. 9 shows that the effective thickness of the hydrocarbon core can be less than 28.6 Å compared to the 32 Å slab thickness where 28.6 Å is determined by the crossover points of the double-bond and water distributions. Although a 3–4 Å difference is not large, it is important to remember that the hydration of our lipids is relatively low. As the hydration is increased, the mean bilayer thickness will decrease and the thermal motion will increase. For DOPC in excess water, S_0 increases to 70 $Å^2$ (Gruner et al., 1988) causing $2D_C$ to decrease to 27 Å. We have been able to observe no more than five diffraction orders from DOPC under these conditions. Using our rule of thumb that the typical full-width of a quasimolecular fragment is d/h_{max} (Wiener and White, 1991a), we can expect the width of the distribution of the double-bond to increase from ~ 8 Å to 12 Å or more depending upon the amount of simple thermal motion relative to the undulatory motion which may be present (see Results). We speculate that there will be a concomitant increase in the width of the water distribution leading to a dynamic thickness considerably smaller than the static one. It would thus appear that for dynamic processes, the effective thickness of bilayers may be much smaller than slab models would indicate.

Epilog

The utility of combining the independent information from neutron and x-ray scattering has long been established in small-molecule (Coppens, 1967, 1974) and protein (Norvell et al., 1975; Wlodawer and Hendrickson, 1982) crystallography. This approach has also been used in structural studies of liquids (Bartsch et al., 1986; Bertagnolli et al., 1988) and glasses (Keen and McGreevy, 1990). A recent paper by Vaknin et al. (1991) demonstrates a useful role for the joint application of neutron and x-ray reflectivity data in the analysis of lipid monolayer structure. Although the joint use of neutron and x-ray diffraction in membrane diffraction has been considered by earlier authors (Kirschner et al., 1975; McCaughn and Krimm, 1982; Herbette et al., 1985), its general application to the solution of bilayer structure has required the systematic reëxamination and further development of theoretical and experimental bilayer diffraction methods (Wiener and White, 1991a–c, 1992; Wiener et al., 1991). We believe that these methods of liquid crystallography may prove to be generally useful in the determination of fluid membrane structure. We speculate that as the method is extended to phospholipids at high hydrations, very significant increases in transbilayer thermal motion and equally significant
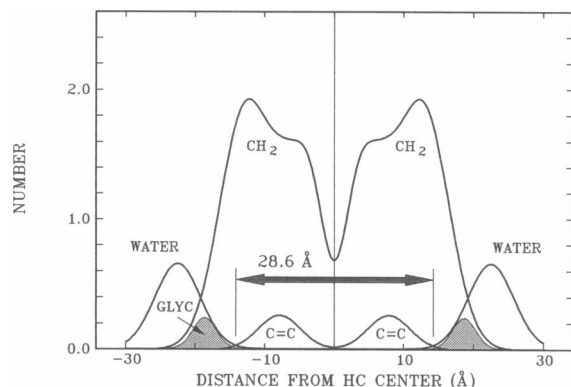
FIGURE 9 Illustration of the methylene/water boundary and the dynamic thickness of a fluid bilayer. The glycerol groups precisely mark the water/methylene boundary for DOPC at 66% RH. The large arrow indicates the minimum instantaneous thickness of the bilayer taken as the transbilayer separation of the extreme edges of the water distributions defined by their intersections with the double-bond distributions. This thickness we define as the dynamic thickness. Here it is 28.6 Å which is several Å smaller than the equivalent hydrocarbon slab thickness (Fig. 8 B). However, as the hydration of the bilayer increases, the dynamic thickness is expected to decrease dramatically. Notice that thermal motion causes a small but significant overlap of the water and double-bond distributions. Petersen (1983) has inferred that a single double-bond dramatically enhances water solubility in hydrocarbons suggesting the possibility of a "ferry" mechanism for water transport. The thermal motion and chemical heterogeneity of the bilayer characterized by the widths and overlaps of the various quasimolecular-fragment Gaussians make it easier to understand how relatively polar molecules may be able to penetrate and cross the bilayer.

decreases in the dynamic thickness of bilayers will be observed. If this speculation proves to be true, it may become easier to understand how seemingly difficult processes such as the transport of proteins into and across membranes can occur.

REFERENCES

Akutsu, H., and T. Nagamori. 1991. Conformational analysis of the polar head group in phosphatidylcholine bilayers: a structural change induced by cations. *Biochemistry.* 30:4510–4516.

Als-Nielson, J. 1987. Solid and liquid surfaces studied by synchrotron x-ray diffraction. *In* Structure and Dynamics of Surfaces II. W. Schommers and P. von Blanckenhagen, editors. Springer-Verlag, Berlin. 181–222.

Als-Nielson, J., and K. Kjaer. 1989. X-ray reflectivity and diffraction studies of liquid surfaces and surfactant monolayers. *In* Phase Transitions in Soft Condensed Matter. T. Riste and D. Sherrington, editors. Plenum Publishing Corp., New York. 113–138.

Aveyard, R., and D. A. Haydon. 1965. Thermodynamic properties of aliphatic hydrocarbon/water interfaces. *Trans. Faraday Soc.* 61:2256–2261.

Bartsch, E., H. Bertagnolli, and P. Chieux. 1986. A neutron and x-ray diffraction study of the binary liquid aromatic system benzene-hexafluorobenzene. II. The mixtures. *Ber. Bunsenges. Phys. Chem.* 90:34–46.

Bertagnolli, H., T. Engelhardt, and P. Chieux. 1988. Structure determining interaction in liquids: an investigation of bromobenzene by x-ray and neutron diffraction experiments. *Ber. Bunsenges. Phys. Chem.* 92:84–91.

Bevington, P. R. 1969. Data Reduction and Error Analysis for the Physical Sciences. McGraw-Hill, New York, 336 pp.

Braach-Maksvytis, V. L. B., and B. A. Cornell. 1988. Chemical shift anisotropies obtained from aligned egg yolk phosphatidylcholine by solid-state ^{13}C nuclear magnetic resonance. *Biophys. J.* 53:839–843.

Büldt, G., H. U. Gally, A. Seelig, J. Seelig, and G. Zaccai. 1978. Neutron diffraction studies on selectively deuterated phospholipid bilayers. *Nature (Lond.).* 271:182–184.

Büldt, G., H. U. Gally, J. Seelig, and G. Zaccai. 1979. Neutron diffraction studies on phosphatidylcholine model membranes. I. Head group conformation. *J. Mol. Biol.* 134:673–691.

Coppens, P. 1967. Comparative x-ray and neutron diffraction study of bonding effects in striazine. *Science (Wash., DC).* 158:1577–1579.

Coppens, P. 1974. Some implications of combined x-ray and neutron diffraction studies. *Acta Cryst.* B30:255–261.

Elder, M., P. Hitchcock, R. Mason, and G. G. Shipley. 1977. A refinement analysis of the crystallography of the phospholipid, 1,2-dilauroyl-DL-phosphatidylethanolamine, and some remarks on lipid–lipid and lipid-protein interactions. *Proc. R. Soc. Lond. A. (Math. Phys. Sci.).* 354:157–170.

Gruner, S. M., M. W. Tate, G. L. Kirk, P. T. C. So, D. C. Turner, D. T. Keane, C. P. S. Tilcock, and P. R. Cullis. 1988. X-ray diffraction study of polymorphic behavior of N-methylated dioleoylphosphatidylethanolamine. *Biochemistry.* 27:2853–2866.

Hauser, H., I. Pascher, R. H. Pearson, and S. Sundell. 1981. Preferred conformation and molecular packing of phosphatidylethanolamine and phosphatidylcholine. *Biochim. Biophys. Acta.* 650:21–51.

Herbette, L., P. DeFoor, S. Fleischer, D. Pascolini, A. Scarpa, and J. K. Blasie. 1985. The separate profile structures of the functional pump protein and the phospholipid bilayer within isolated sarcoplasmic reticulum membranes determined by x-ray and neutron diffraction. *Biochim. Biophys. Acta.* 817:103–122.

Hitchcock, P. B., R. Mason, K. M. Thomas, and G. G. Shipley. 1974. Structural chemistry of 1,2-dilauroyl-DL-phosphatidylethanolamine: Molecular conformation and intermolecular packing of phospholipids. *Proc. Natl. Acad. Sci. USA.* 71:3036–3040.

Hübner, W., and H. H. Mantsch. 1991. Orientation of specifically ^{13}C=O labeled phosphatidylcholine multilayers from polarized attenuated total reflection FT-IR Spectroscopy. *Biophys. J.* 59:1261–1272.

Jacobs, R. E., and S. H. White. 1989. The nature of the hydrophobic binding of small peptides at the bilayer interface: implications for the insertion of transbilayer helices. *Biochemistry.* 28:3421–3437.

Keen, D. A., and R. L. McGreevy. 1990. Structural modelling of glasses using Monte Carlo simulation. *Nature (Lond.).* 344:423–425.

King, G. I., R. E. Jacobs, and S. H. White. 1985. Hexane dissolved in dioleoyllecithin bilayers has a partial molar volume of approximately zero. *Biochemistry.* 24:4637–4645.

King, G. I., and S. H. White. 1986. Determining bilayer hydrocarbon thickness from neutron diffraction measurements using strip-function models. *Biophys. J.* 49:1047–1054.

Kirschner, D. A., D. L. D. Caspar, B. P. Schoenborn, and A. C. Nunes. 1975. Neutron diffraction studies of nerve myelin. *Brookhaven Symp. Biol.* 27:III68–III76.

Lewis, B. A., and D. M. Engelman. 1983. Lipid bilayer thickness varies linearly with acyl chain length in fluid phosphatidylcholine vesicles. *J. Mol. Biol.* 166:211–217.

Luzzati, V. 1968. X-ray diffraction studies of lipid-water systems. *In* Biological Membranes. D. Chapman, editor. Academic Press, New York. 71–123.

Luzzati, V., and F. Husson. 1962. The structure of the liquid-crystalline phases of lipid-water systems. *J. Cell Biol.* 12:207–219.

McCaughn, L., and S. Krimm. 1982. Biochemical profiles of membranes from x-ray and neutron diffraction. *Biophys. J.* 37:417–426.

McIntosh, T. J., and S. A. Simon. 1986. Hydration force and bilayer deformation: a reevaluation. *Biochemistry.* 25:4058–4066.

McIntosh, T. J., A. D. Magid, and S. A. Simon. 1987. Steric repulsion between phosphatidylcholine bilayers. *Biochemistry.* 26:7325–7332.

Nagle, J. F., and M. C. Wiener. 1988. Structure of fully hydrated bilayer dispersions. *Biochim. Biophys. Acta.* 942:1–10.

Norvell, J. C., A. C. Nunes, and B. P. Schoenborn. 1975. Neutron diffraction analysis of myoglobin: Structure of the carbon monoxide derivative. *Science (Wash., DC).* 190:568–570.

Petersen, D. C. 1983. The water permeability of the monolein/triolein bilayer membrane. *Biochim. Biophys. Acta.* 734:201–209.

Press, W. H., B. P. Flannery, S. A. Teukolsky, and W. T. Vetterling. 1986. Numerical Recipes. The Art of Scientific Computing. Cambridge University Press, Cambridge, United Kingdom. 702 pp.

Rand, R. P., and V. A. Parsegian. 1989. Hydration forces between phospholipid bilayers. *Biochim. Biophys. Acta.* 988:351–376.

Requena, J., and D. A. Haydon. 1975. Van der Waals forces in oil-water systems from the study of thin lipid films. II. The dependence of the van der Waals free energy of thinning on film composition and structure. *Proc. R. Soc. Lond. A. (Math. Phys. Sci.).* 347:161–177.

Safinya, S. 1989. Rigid and fluctuating surfaces: A series of synchrotron x-ray scattering studies of interacting stacked membranes. *In* Phase Transitions in Soft Condensed Matter. T. Riste and D. Sherrington, editors. Plenum Publishing Corp., New York. 249–270.

Scherer, J. R. 1989. On the position of the hydrophobic/hydrophilic boundary in lipid bilayers. *Biophys. J.* 55:957–964.

Sears, V. F. 1986. Neutron scattering lengths and cross-sections. *In* Neutron Scattering, Pt. A. (Methods and Experimental Physics. Vol. 23). K. Sköld and D. L. Price, editors. Academic Press, New York. 521–550.

Sirota, E. B., C. R. Safinya, R. J. Plano, and N. A. Clark. 1988. X-ray scattering studies of aligned, stacked surfactant membranes. *Science (Wash., DC).* 242:1406–1409.

Small, D. M. 1967. Phase equilibria and structure of dry and hydrated egg lecithin. *J. Lipid. Res.* 8:551–557.

Small, D. M. 1986. The Physical Chemistry of Lipids. Plenum Press, New York. 672 pp.

Smith, G. S., C. R. Safinya, D. Roux, and N. A. Clark. 1987. X-ray studies of freely suspended films of a multilamellar lipid system. *Mol. Cryst. Liq. Cryst.* 144:235–255.

Strenk, L. M., P. W. Westerman, and J. W. Doane. 1985. A model of orientational ordering in phosphatidylcholine bilayers based on conformational analysis of the glycerol backbone region. *Biophys. J.* 48:765–773.

Tardieu, A., V. Luzzati, and F. C. Reman. 1973. Structure and polymorphism of the hydrocarbon chains of lipids: A study of lecithin-water phases. *J. Mol. Biol.* 75:711–733.

Vaknin, D., K. Kjaer, J. Als-Nielsen, and M. Lösche. 1991. Structural properties of phosphatidylcholine in a monolayer at the air/water interface. A neutron reflection study and reexamination of x-ray reflection measurements. *Biophys. J.* 59:1324–1332.

Warren, B. E. 1969. X-ray Diffraction. Addison-Wesley, Reading, Massachusetts. 381 pp. (Reprinted by Dover Publications, New York, 1990).

Weast, R. C., editor. 1981. CRC Handbook of Chemistry and Physics. (62nd Ed.) CRC Press, Inc.., Boca Raton, FL.

White, S. H., and G. I. King. 1985. Molecular packing and area compressibility of lipid bilayers. *Proc. Natl. Acad. Sci. USA.* 82:6532–6536.

White, S. H., R. E. Jacobs, and G. I. King. 1987. Partial specific volumes of lipid and water in mixtures of egg lecithin and water. *Biophys. J.* 52:663–665.

Wiener, M. C., G. I. King, and S. H. White. 1991. The structure of a fluid dioleoylphosphatidylcholine bilayer determined by joint refinement of x-ray and neutron diffraction data. I. Scaling of neutron data and the distributions of double bonds and water. *Biophys. J.* 60:568–576.

Wiener, M. C., and S. H. White. 1991a. Fluid bilayer structure determination by the combined use of x-ray and neutron diffraction. I. Fluid bilayer models and the limits of resolution. *Biophys. J.* 59:162–173.

Wiener, M. C., and S. H. White. 1991b. Fluid bilayer structure determination by the combined use of x-ray and neutron diffraction. II. The "composition space" refinement method. *Biophys. J.* 59:174–185.

Wiener, M. C., and S. H. White. 1991c. The transbilayer distribution of bromine in fluid bilayers containing a specifically brominated analog of dioleoylphosphatidylcholine. *Biochemistry.* 30:6997–7008.

Wiener, M. C., and S. H. White. 1992. Structure of a fluid dioleoylphosphatidylcholine bilayer determined by joint refinement of x-ray and neutron diffraction data. II. Distribution and packing of terminal methyl groups in a fluid lipid bilayer. *Biophys. J.* 61:428–433.

Wlodawer, A., and W. A. Hendrickson. 1982. A procedure for joint refinement of macromolecular structures with x-ray and neutron diffraction from single crystals. *Acta Cryst.* A38:239–247.

Zaccai, G., G. Büldt, A. Seelig, and J. Seelig. 1979. Neutron diffraction studies on phosphatidylcholine model membranes. II. Chain conformation and segmental disorder. *J. Mol. Biol.* 134:693–706.